

Resolving the Evolution of Iron in the ICM: Dissecting the Iron Mass Budget into Multiple Components

Ang Liu^{1,2,3}, Paolo Tozzi¹, Stefano Ettori^{4,5}, Sabrina De Grandi⁶, Fabio Gastaldello⁷, Piero Rosati⁸, Colin Norman⁹

¹ INAF - Osservatorio Astrofisico di Arcetri, Largo E. Fermi, I-50122 Firenze, Italy [liuang@arcetri.astro.it]

² Department of Physics, Sapienza University of Rome, I-00185 Rome, Italy

³ Department of Physics, University of Rome Tor Vergata, I-00133, Rome, Italy

⁴ INAF - Osservatorio di Astrofisica e Scienza dello Spazio, via Pietro Gobetti 93/3, 40129 Bologna, Italy

⁵ INFN, Sezione di Bologna, viale Berti Pichat 6/2, I-40127 Bologna, Italy

⁶ INAF - Osservatorio Astronomico di Brera, Via E. Bianchi, 46, I-23807 Merate (LC), Italy

⁷ INAF - Istituto di Astrofisica Spaziale e Fisica cosmica di Milano

⁸ Dipartimento di Fisica e Scienze della Terra, Università degli Studi di Ferrara, via Saragat 1, I-44122 Ferrara, Italy

⁹ Department of Physics and Astronomy of the Johns Hopkins University, 3400 N. Charles Street, Baltimore, MD 21218, USA

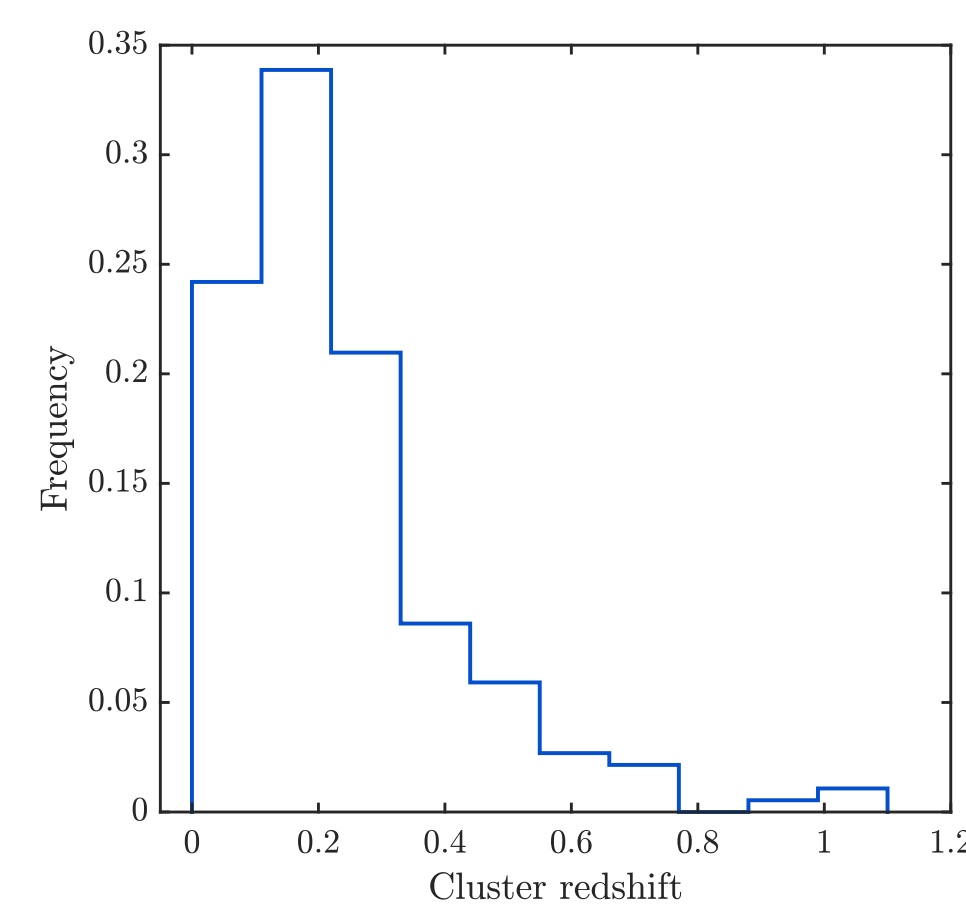
(We acknowledge financial contribution from the agreement ASI-INAF n.2017-14-H.0)

Abstract

Mixed results have been obtained in the past decades on the chemical evolution of the intracluster medium [1,2,3,4]. One reason is that the spatial distribution of metals (among which iron is the most prominent and observable up to high z in the X-ray band), which may significantly affect the measurement of average metallicity, is not fully investigated. To solve this problem, we make the first attempt to dissect the iron abundance profiles into two components, a central peak and a large-scale plateau, and explore their evolution separately. Our results are consistent with the early-enrichment picture that most of the iron in the ICM is produced at early epochs [5], and present little evolution from redshift 1 to 0. On the other hand, we find a weak evolutionary signal in the more recently formed central iron peak, which only contributes a few percent to the total iron mass. We also show that the apparent factor of 2 evolution from $z=1$ to $z=0$ previously observed is a complex result of the use of emission weighted values coupled with some evolution in the central iron peak, and the selection of cluster sample.

Sample and Data

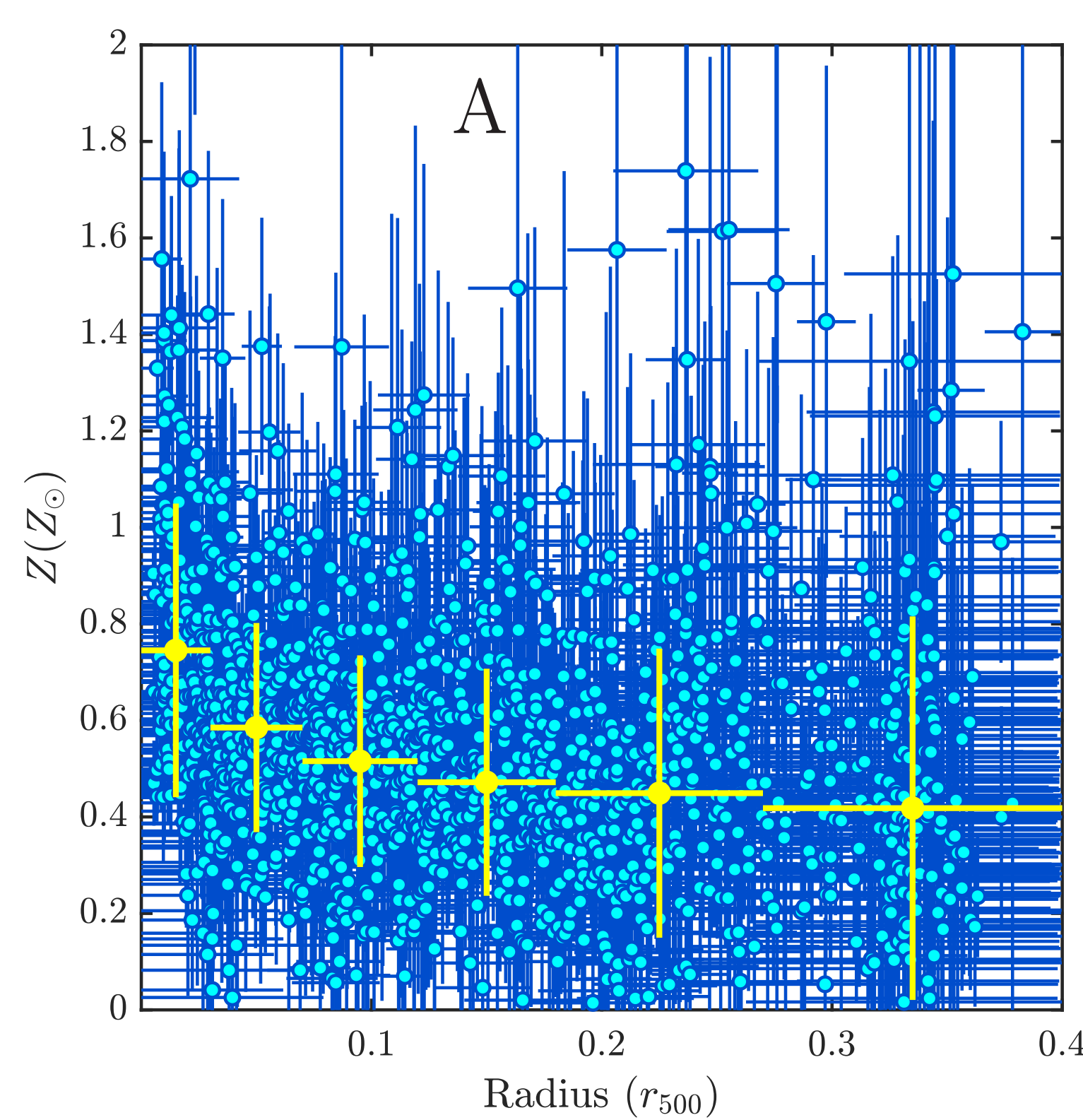
We start from a list of galaxy clusters with *Chandra* archival observations. Our aim is to identify and disentangle spatial components assumed to have spherical symmetry. Clearly, this puts a strong constraint on the morphology of clusters suitable for our analysis. Starting from a total of ~ 500 targets in the *Chandra* data archive, we obtain a final sample consisting of 186 clusters, spreading over a redshift range [0.04, 1.07].



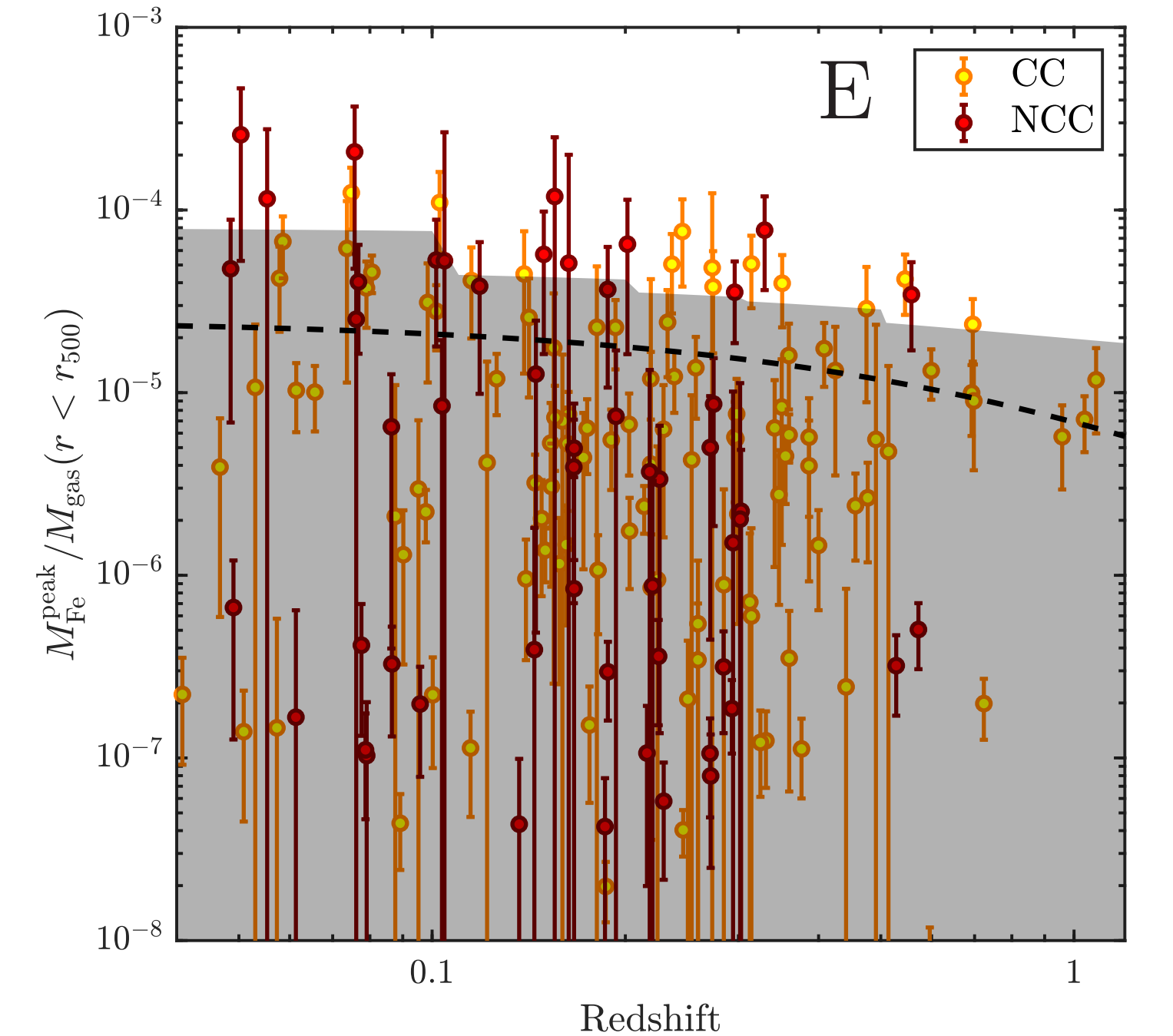
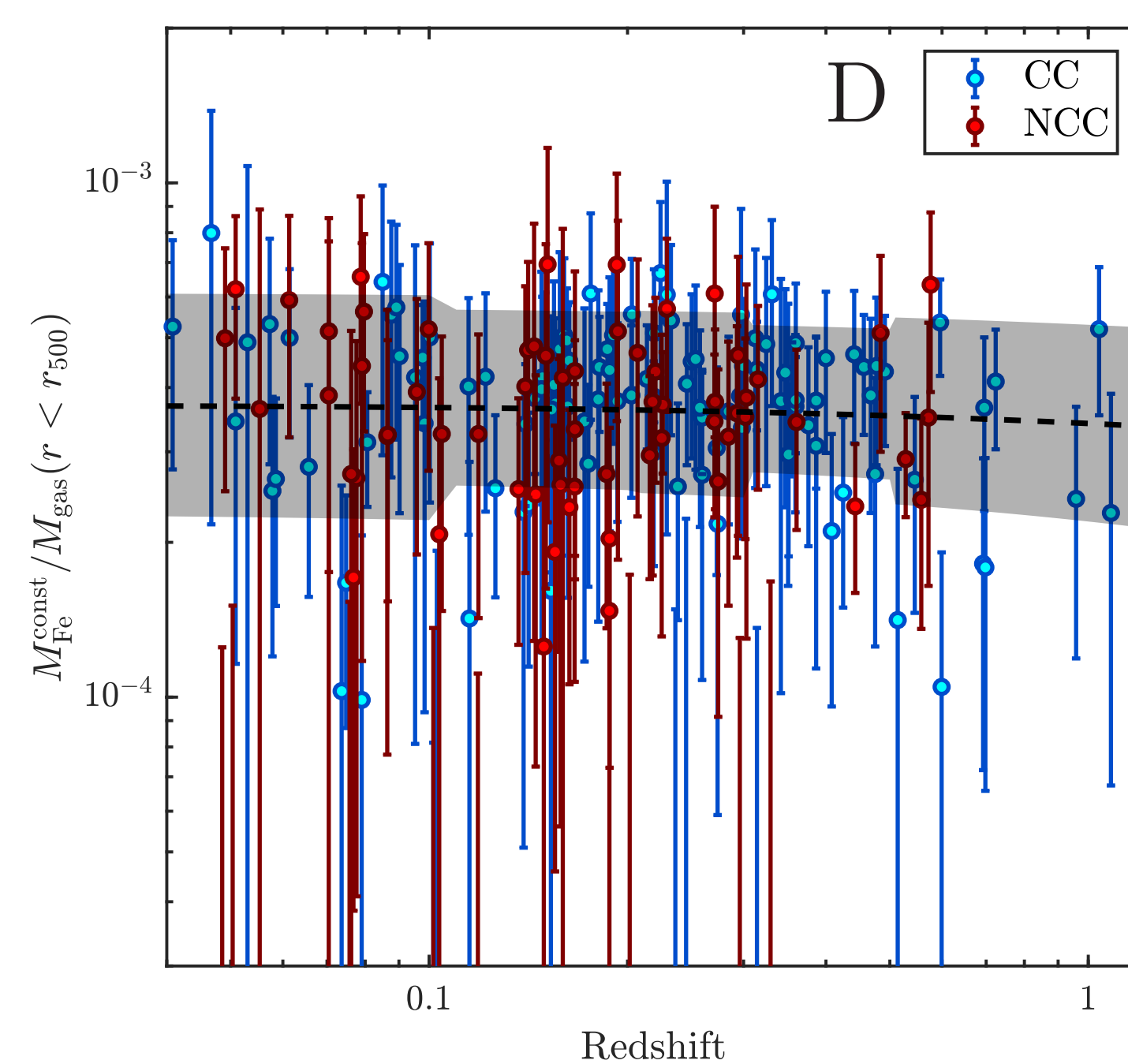
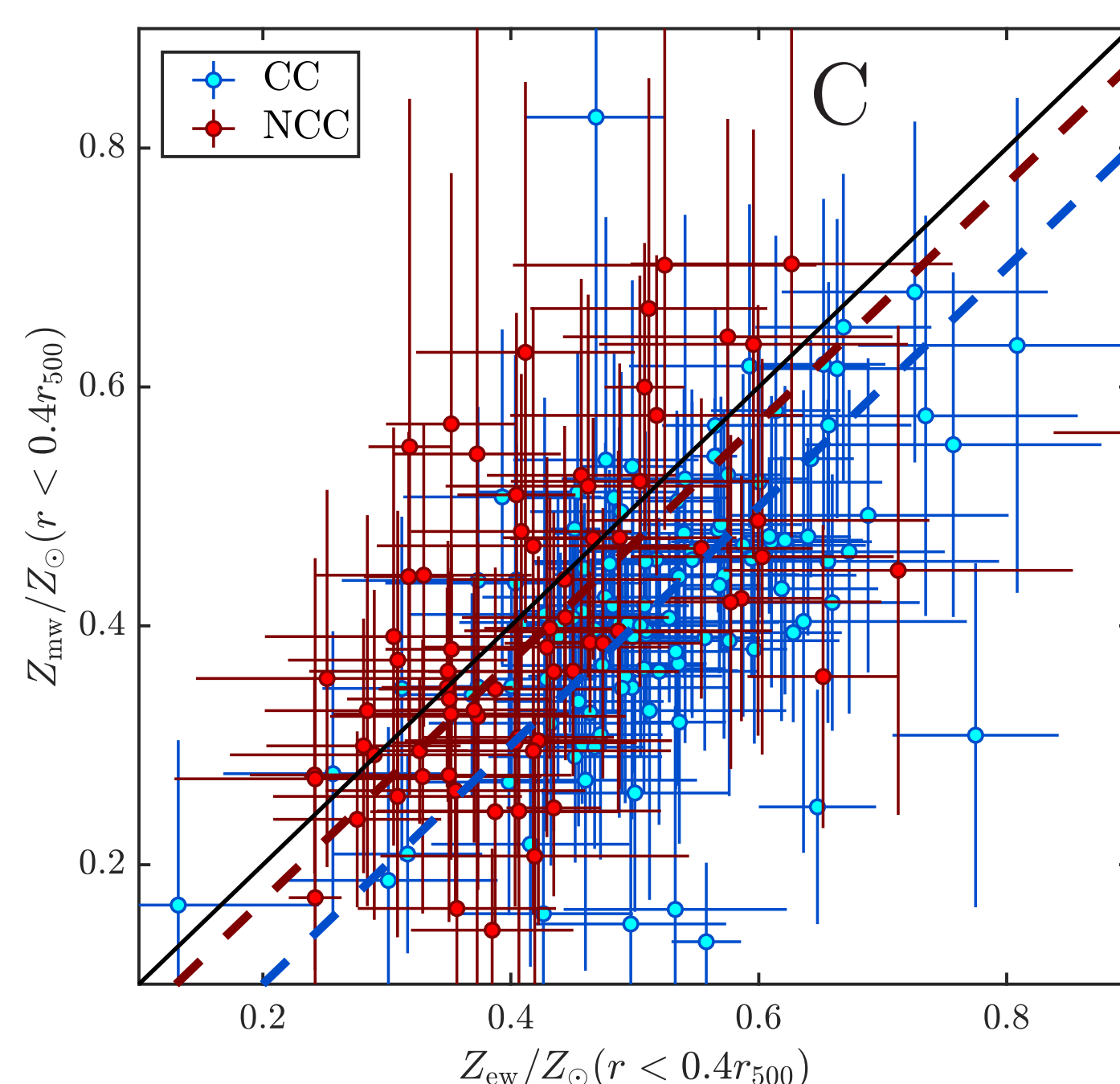
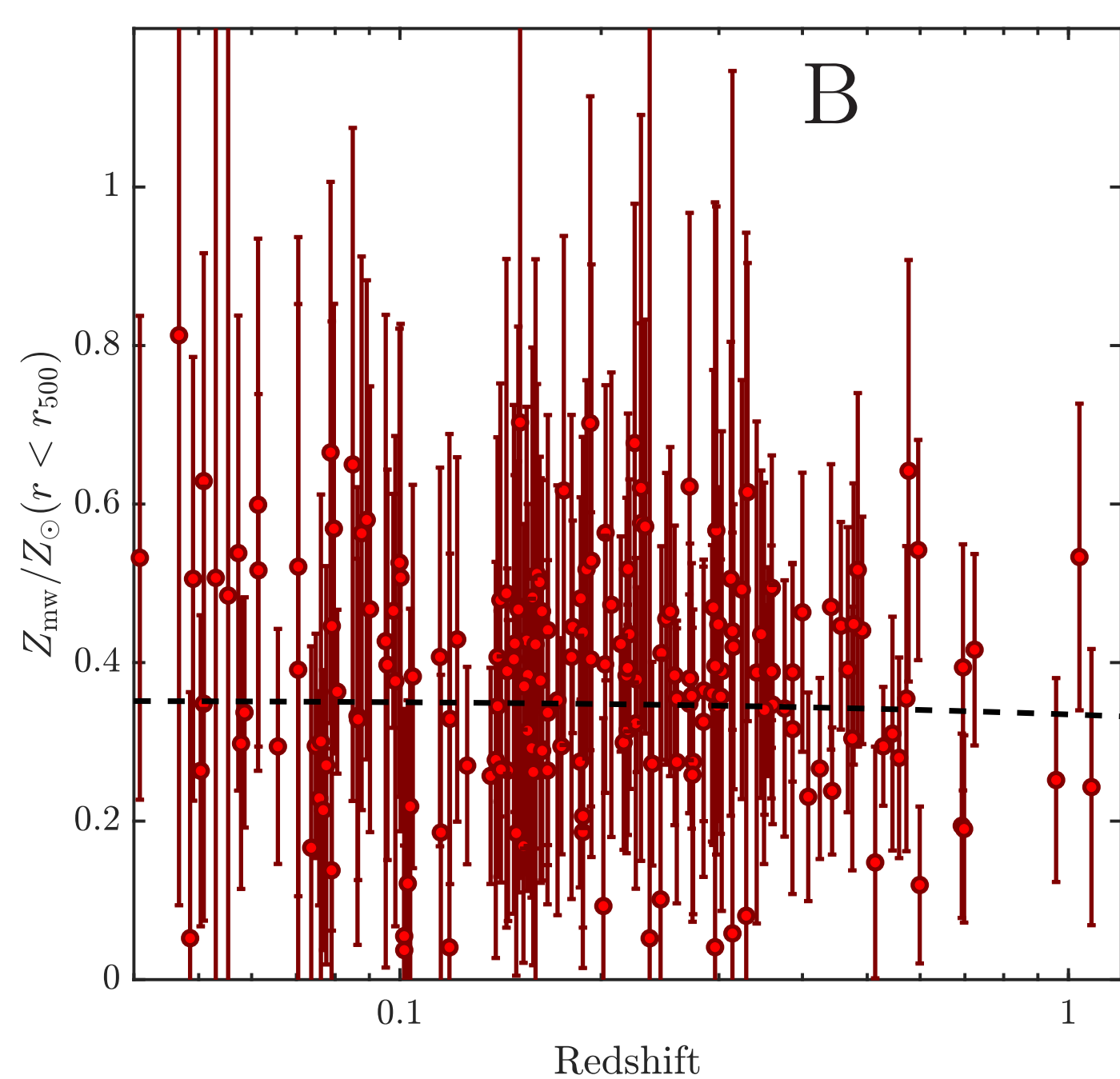
Method

For each cluster, we measure the profiles of iron abundance, gas density, iron mass, and the mass-weighted iron abundance. We fit the abundance profiles with a double-component model, consisting of a central peak probably formed due to the more recent star formation in the central galaxy, and an approximately constant plateau reaching the largest radii, associated with early enrichment occurred before and/or shortly after the formation of the cluster.

Main results



- ▶ The azimuthally-averaged iron abundance profiles of all the clusters in our sample. (Fig. A)
- ▶ The average mass-weighted iron abundance within r_{500} without resolving the two components. The best-fit function of the distribution gives $Z_{mw} = Z_{mw,0} \cdot (1+z)^{-\gamma}$ with $\gamma = 0.08 \pm 0.17$, consistent with no evolution of Z_{mw} across our sample. (Fig. B)
- ▶ The mass-weighted abundance within $0.4r_{500}$ plotted against the emission-weighted value in the same radial range. Blue and red dots denote cool-core and non-cool-core clusters, and the dashed lines show the average discrepancies of this two classes of clusters, $Z_{mw}^{CC} = Z_{ew} - 0.10$ and $Z_{mw}^{NCC} = Z_{ew} - 0.03$. The difference in CC and NCC clusters reflects the effect of the iron peak on the measurement of emission-weighted abundance. (Fig. C)
- ▶ Iron mass of the plateau and the peak within r_{500} (divided by gas mass) versus cluster redshift. Shaded area indicates the scatter of the distribution. Both components do not show an indication of evolution in mass, although the iron peak shows a decrease with redshift. The iron peak mass exhibits an extremely large intrinsic scatter, in line with the fact that it is produced after the virialization of the halo and depends on the formation of a cool core and the strength of the feedback. (Fig. D&E)



Conclusions

We identify two components in the iron distribution in most of the clusters in our sample, including an iron peak in the center, and an approximately constant plateau across the entire cluster. Our results suggest that the majority of iron mass in the ICM of massive galaxy clusters is produced at epochs earlier than $z \sim 1$, probably during the star formation peak at $z \sim 2$. On the other hand, the iron peak component, despite contributing a minority fraction in the total iron mass, shows a low significance decrease with redshift and an extremely large intrinsic scatter. In general, our results confirm the early-enrichment scenario suggested by recent works [4,5], and suggest that the evolution from $z=1$ to $z=0$ previously observed [1,2] is partially due to the use of emission weighted values and some evolution in the iron peak. Due to the incompleteness of our sample, we can not make further definitive conclusions on the evolution of iron. We will eventually extend this study with two-component modelization to complete samples.

References

- [1] Balestra, I., et al., 2007, A&A, 462, 429; [2] Maughan, B. J., et al., 2008, ApJS, 174, 117; [3] Ettori, S., et al., 2015, A&A, 578, A46; [4] McDonald, M., et al., 2016, ApJ, 826, 124; [5] Mantz, A. B., et al., 2017, MNRAS, 472, 2877; [6] Liu, A., et al., 2018, MNRAS, 481, 361.